

## **A 16 kyr record of ocean circulation and monsoon intensification from the central Bay of Bengal**

**Sushant S. Naik<sup>\*1</sup>, Chandranath Basak<sup>2†</sup>, Steven L. Goldstein<sup>2,3</sup>, P. Divakar Naidu<sup>1</sup>, and Smita N. Naik<sup>1</sup>**

1 CSIR-National Institute of Oceanography, Goa 403004, INDIA

2 Lamont-Doherty Earth Observatory of Columbia University, Palisades, NY 10964, USA

3 Department of Earth and Environmental Sciences, Columbia University, Palisades, NY 10964, USA

\* Corresponding author: Sushant Naik (sushant@nio.org)

† Now at California State University, Bakersfield, CA 93311, USA

### **Key Points:**

- Nd isotopes are used as a water mass tracer in the Bay of Bengal.
- The Global Overturning Circulation controlled the deep circulation in the Bay of Bengal for the major portion of the last deglaciation.
- After 8-7 ka, the weathering signal due to enhanced monsoon activity has overwhelmed the deep ocean circulation signal in the central Bay of Bengal.

### **Abstract**

The monsoonal signal dominates most climate records from the Indian Ocean. As a consequence, conventional stable isotope tracers have not been effective at tracking ocean circulation in the Indian Ocean, and distinguishing between monsoonal and ocean circulation changes in the Bay of Bengal. Here we present a deglacial through Holocene Nd isotope record of seawater in the central Bay of Bengal, spanning the last 16 kyr. Comparison with a published record from the deep equatorial Indian Ocean (Piotrowski et al., 2009) shows that Nd isotope ratios of these cores were similar until ~8 ka ( $\epsilon_{Nd} = -7$  to  $-8$  until ~13 ka, and  $-8.5$  to  $-9.5$  between ~13 and 8 ka), after which the Bay of Bengal record diverges to lower values ( $\epsilon_{Nd} = \sim -10.5$ ). We interpret the Nd isotope record until ~8 ka in both cores to represent the influence of the global overturning ocean circulation. The divergence of the record in the Bay of Bengal since ~8 ka to lower  $\epsilon_{Nd}$ -values is coincident with a major increase in the strength of the rain-bearing southwest monsoon, and a high sediment load from the Ganga-Brahmaputra Rivers to the Bengal Fan that reflects major impacts from the intensified monsoon. Thus the Nd isotopes are sensitive recorders of the changes in monsoon intensity in the Bay of Bengal.

**Keywords:** neodymium isotopes, foraminifera, Bay of Bengal, global overturning circulation, monsoon, deglaciation.

## 1. Introduction

The climate in and around Indian Ocean, with large embayments on both sides of India (the Arabian Sea and the Bay of Bengal (BoB)), is heavily influenced by the Indian monsoon. The presence of the Himalayas – the highest and most active orogenic belt in the world, yielding abundant runoff due to the southwest (SW) Indian monsoon by a large network of active rivers – make the BoB a key location to study past changes in weathering and monsoonal intensity. Burton and Vance (2000) reported glacial-interglacial variations in Nd isotopes in cleaned foraminifera and bulk sediments in ODP Site 758 (Figure 1a), from the northern end of the Ninetyeast Ridge in the central BoB over the last ~150 ka. They concluded that the Nd isotope variations reflect the fluctuations of riverine input to the BoB in phase with changes in global climate cycles, here associated with increased SW monsoon activity during interglacials. Multiple studies have indicated the existence of atmospheric teleconnections between cold events in the North Atlantic and weak Indian monsoons (Schulz et al., 1998; Kudrass et al., 2001; Marzin et al., 2013). Gourlan et al. (2010) interpreted Nd isotope variations in carbonates from the northern BoB over the last 4 million years, also from Site 758, as a mixture of contributions from riverine discharge and BoB seawater, and concluded that a close relationship exists between SW monsoon-dominated riverine discharge and northern hemispheric climate changes. However, along with the monsoonal signal, the signal from the global overturning circulation is an important contributor to the Indian Ocean, especially to the deep ocean, and in the BoB it has been a challenge to distinguish between these two contributions.

Here we address the issue of distinguishing the ocean circulation and monsoon signals using downcore Nd isotopes in Fe-Mn encrusted foraminifera from deep sea core SK 157-20 (12°09'N; 88°42'E) recovered at 3171 m water depth in the central BoB (Figure 1a). Our data are evaluated in the context of present-day seawater Nd isotopes in the region (Singh et al., 2012; Yu et al., 2017), an authigenic Nd isotope time series from the equatorial deep Indian Ocean away from the BoB (Piotrowski et al., 2009), and other published authigenic  $\epsilon_{Nd}$  data from the BoB. Outstanding questions pertinent to deep ocean circulation in the central BoB and Indian SW monsoonal variations include the following: (i) can we use Nd isotopes as a water mass tracer during periods of weak SW monsoon in the BoB; (ii) if Nd isotopes record water mass mixing during periods of low monsoon intensity, what was the BoB deep-water circulation like; (iii) when did the hydrogenous Nd isotopic signature of deep BoB transition from a global overturning circulation dominated basin to one dominated by the monsoon?

## 2. Hydrography

Unlike the North Atlantic, the Indian Ocean has no active deep-water formation in the north, and the large-scale Indian Ocean circulation pattern can be summarized in terms of the net northward inflow at depth, and relatively passive southward outflow in the upper ocean. A large portion of intermediate, deep and bottom water in the Indian Ocean is composed of the Antarctic Intermediate Water (AAIW), Antarctic Bottom Water (AABW), and Modified North Atlantic Deep Water (MNADW) (Wyrki, 1973). In the northern Indian Ocean, North Indian Deep Water (NIDW) is produced by sinking of Persian Gulf Water and Red Sea Water, followed by mixing with northward flowing Circumpolar-derived waters. Both MNADW and NIDW have high salinity and are referred to as High Salinity Deep Waters (HSDW) (Kumar and Li, 1996). Below depths of  $\sim 3$  km, HSDW is the major water mass, followed by AABW, with more AABW entering the BoB than the Arabian Sea (Kumar and Li, 1996). Waters shallower than 1000 m in the BoB are mainly composed of the following components: Ganga-Brahmaputra dominated low salinity water, BoB sub-surface water, Arabian Sea high salinity water, Indonesian Throughflow water and north Indian intermediate water (Kumar and Li, 1996). The location of deep sea core SK 157-20 (Figure 1a) in the central BoB is currently situated north of the pure AABW realm and in a mixture of AABW and MNADW ( $\epsilon_{Nd} = \sim -10.5 - 11$ ; Singh et al., 2012) (Figure 1b).

## 3. Nd isotopes in the global oceans and the Bay of Bengal

Over the last couple of decades, Nd isotopes have become increasingly used as a tracer of deep ocean circulation (e.g. Goldstein and Hemming 2003, van de Flierdt et al., 2016, and refs. therein), based on observations that seawater samples below the thermocline in many regions of the oceans show ‘conservative behavior’, that is, to a first order reflecting the values predicted from mixing of North Atlantic- and Pacific-sourced water masses (with North Atlantic Deep Water or NADW having  $\epsilon_{Nd} = \sim -13.5$  and North Pacific Deep Water or NPDW having  $\epsilon_{Nd} = \sim -4$ , where  $\epsilon_{Nd}$  is the deviation, in parts per 10,000, from the average silicate earth as estimated from chondritic meteorites (Jacobsen and Wasserburg, 1980). This observation that Nd isotopes show largely conservative behavior holds in many parts of the oceans despite the potential to change the  $\epsilon_{Nd}$ -values through Nd input from regional sources. As in many parts of the oceans, Nd isotopes behave non-conservatively at shallow depths, while these effects are not seen in the deep oceans (Goldstein and Hemming, 2003). For example, Yu et al. (2017) reported significant seasonal variations in dissolved Nd isotopes (up to 2  $\epsilon_{Nd}$ -units) in the shallow BoB, while variations observed below  $\sim 2000$  m (of  $\sim 0.5$   $\epsilon_{Nd}$ -units) are close to the long-term external reproducibility of that study. Nevertheless, in the BoB, the behavior of Nd isotopes has been reported to be non-conservative. Singh et al. (2012) reported dissolved Nd isotopes

along 87°E in the BoB as impacted by Nd from particulate phases of Ganga-Brahmaputra (G-B) rivers, such that the deep seawater values are offset from water mass mixing, making Nd isotopes inapplicable as a global ocean water mass tracer. However, while G-B riverine particulates are an important contributor to the modern Nd budget of the BoB, it is largely unknown how the paleo seawater Nd isotope record was affected by monsoonal intensity and associated river borne continental particle fluxes (e.g., G-B vs. SE Asian rivers). A proper evaluation of the influence of the continental input on the hydrogenous  $\epsilon_{Nd}$  signal in the BoB in the past is necessary in order to decipher the viability of Nd isotopes as a paleo-water mass tracer or a SW monsoon tracer in this marginal setting.

#### 4. Materials and Methods

Core SK 157-20 (12.15°N, 88.7°E; water depth 3171 m) was collected during an expedition onboard R/V Sagar Kanya in the central BoB in October 2000. Sediment samples were wet sieved at Council of Scientific and Industrial Research (CSIR)-National Institute of Oceanography (NIO), Goa, and the size fraction  $> 125 \mu\text{m}$  was used for separating foraminifera and fossil fish teeth/broken bone fragments ('fish debris' from here on). Planktonic foraminifera *Globigerinoides ruber* (250 to 350  $\mu\text{m}$  size range) have been used to generate a downcore  $\delta^{18}\text{O}$  record. Stable isotopic measurements were performed using a Finnigan MAT 252 mass spectrometer equipped with an automatic carbonate preparation device at the University at Bremen, Germany (Naik and Naidu, 2016). The long-term reproducibility ( $1\sigma$  over a one year period) derived from replicate measurements of carbonate standards (National Bureau of Standards 18, 19 and 20) is better than  $\pm 0.07\text{‰}$  for  $\delta^{18}\text{O}$ .

Nd isotope measurements were performed at Lamont-Doherty Earth Observatory of Columbia University (LDEO). The downcore Nd isotopic record has been generated using mixed species of Fe-Mn encrusted planktic and benthic foraminifera, cleaned of terrigenous detritus, which previous studies show preserves the deep seawater signal (e.g., Roberts et al., 2010). All foraminifera samples were subjected to physical cleaning, involving gently crushing the foram tests with glass slides to break open the inner chamber before they were subjected to multiple rinses and sonication in Optima<sup>®</sup> grade methanol and deionized water (e.g. Wilson et al., 2012; Pena et al., 2013). The cleaned broken foraminifer fragments were examined under a binocular microscope to ensure that no clay fragments remained in the sample. The cleaned, crushed foraminifera were dried and dissolved in  $<10\%$  acetic acid for 5-10 min. The dissolved solution was centrifuged and the supernatant was dried down and re-dissolved in 1N  $\text{HNO}_3$ . Eichrom TRU-spec<sup>®</sup> resin (particle size 100-150  $\mu\text{m}$ ) was used to separate rare earth elements (REEs) from other major cations. Nd was further purified with LN-spec resin (particle size 50-10  $\mu\text{m}$ ) using 0.25 N HCl as eluent. The Nd fraction was dried and treated with a 1:1 mixture of  $\text{H}_2\text{O}_2$  (30%) and concentrated  $\text{HNO}_3$  to breakdown organic compounds that may have leaked during

column chemistry. The final Nd aliquot was brought up in 2% HNO<sub>3</sub> and analyzed for Nd isotopes using a Thermo Scientific Neptune Plus<sup>®</sup> multi-collector inductively coupled plasma mass spectrometer (MC-ICPMS) at LDEO. The international standard JNdi-1 was analyzed after each sample and all reported <sup>143</sup>Nd/<sup>144</sup>Nd ratios (Table 1) were normalized to a JNdi-1 value of 0.512115 (Tanaka et al., 2000) using the mean <sup>143</sup>Nd/<sup>144</sup>Nd of the JNdi-1 measurements of each analytical session. Typical external reproducibility on a 20 ppb JNdi-1 solution is generally better than ±0.3 ε<sub>Nd</sub> units (2σ). ε<sub>Nd</sub> values reported are the fractional deviation in parts per 10,000 from the average <sup>143</sup>Nd/<sup>144</sup>Nd value of chondritic meteorites (0.512638) as estimated by Jacobsen and Wasserburg (1980).

## 5. Results

The age model of SK 157-20 is based on 5 radiocarbon ages (Naik and Naidu, 2016) as well as correlation between the δ<sup>18</sup>O record of planktic foraminifera *G. ruber* with that of a reference core, 126 KL from the northern BoB (Kudrass et al., 2001) (Figure 1a). The average sedimentation rate for the past 16 ka is 4 cm/kyr and the age uncertainty is on the order of ~ ±200 yr.

The SK 157-20 core top represents sediment of Holocene age with an ε<sub>Nd</sub>-value of -10.4, which is in agreement within analytical uncertainty with deep water from a nearby station (ε<sub>Nd</sub> = -10.5; Station 809, 13.77°N, 87°E; Singh et al., 2012) (Table 1; Figure 1b), thus providing evidence that foraminifera-derived Nd isotope values in SK 157-20 reliably records the ambient deep seawater in the central BoB. Because fossil fish debris have been shown to be particularly robust recorders of paleo-seawater (e.g., Martin and Scher, 2004), we analyzed fish debris from a sediment interval for which the foraminifera derived ε<sub>Nd</sub>-value is available (Figure 2a). The agreement between fish debris (ε<sub>Nd</sub> = -10.7) and the foraminifera derived value (ε<sub>Nd</sub> = -10.6) provides further evidence that the foraminifera-derived ε<sub>Nd</sub> downcore record represents the bottom water ε<sub>Nd</sub> signature and not an artifact due to contamination from lithogenic contributions.

The ε<sub>Nd</sub>-values of the time series range between -7.1 and -10.6 (Figure 2a), with higher values during the deglacial interval (16.5 – 11 ka) and lower values during the Holocene. Throughout Heinrich Stadial 1 (HS1) the ε<sub>Nd</sub>-value remained ~ -7.6 to -8.0 and began to decrease at the end of the Bølling-Ållerød (B-A). The trend of decreasing ε<sub>Nd</sub>-values continued through the YD and stabilized at an average value of ~ -9 by the end of YD, which lasted until ~8 ka. At that time the ε<sub>Nd</sub>-value increased to ~ -10.5 and has remained so for the rest of the duration of Holocene.

The δ<sup>18</sup>O of calcite (δ<sup>18</sup>O<sub>C</sub>) of *Globigerinoides ruber* in SK 157-20 reported here are in the range between -0.69 to -2.91‰ with an overall decreasing trend that continued until the beginning of

the Holocene (Table 1; Figure 2b). In detail, the  $\delta^{18}\text{O}$  record shows maximum values during the HS1, decreases in  $\delta^{18}\text{O}$  by  $\sim 1\text{‰}$  during the B-A, and further decreases after Younger Dryas (YD) to an average value  $\sim -2.6\text{‰}$ . This average persisted through the Holocene until  $\sim 6$  ka, when it slightly increased (Figure 2b). In order to reconstruct  $\delta^{18}\text{O}$  of seawater ( $\delta^{18}\text{O}_{\text{SW}}$ ) in the central BoB, we have corrected  $\delta^{18}\text{O}_{\text{c}}$  of *G. ruber* for ice volume (Waelbroeck et al., 2003). In the absence of any absolute sea surface temperature (SST) record from SK 157-20, we used nearby western BoB core SK218 (Govil and Naidu, 2011) ( $14.03^{\circ}\text{N}$ ,  $82^{\circ}\text{E}$ ; water depth 3307m; Figure 1a) to calculate the temporal variation of  $\delta^{18}\text{O}_{\text{SW}}$  in the central BoB (Figure 2c) based on Bemis et al., (1998). SST changes in the BoB during the last glaciation hardly exceeded  $\sim 3^{\circ}\text{C}$  (e.g., Rashid et al., 2007; Kudrass et al., 2001; Govil and Naidu, 2011), which produces only a  $\sim 0.65\text{‰}$  change in  $\delta^{18}\text{O}_{\text{c}}$ , much smaller than the  $\sim 2\text{‰}$  change observed in our record. Thus, changing SST in the western BoB would not explain the millennial scale variability that we observe in our record. Rather we argue, our  $\delta^{18}\text{O}_{\text{SW}}$  record is best explained as changes in salinity.

## 6. Discussion

The total annual continental runoff into the BoB is  $2950 \text{ km}^3$ , the majority of which is during the summer (SW) monsoon (Sengupta et al., 2006). The fresh water flux to the BoB via high runoff and rainfall far exceeds moisture loss due to evaporation, and thus controls the salinity budget in the BoB (Duplessy, 1982; Rashid et al., 2007). Further, the northern BoB is particularly sensitive to salinity changes as a result of varying hydrological conditions due to its proximity to the G-B. A salinity record, from core 126 KL recovered near the mouth of the G-B in the northern BoB ( $19.98^{\circ}\text{N}$ ,  $90.03^{\circ}\text{E}$ ; water depth 1253m) reflects outflow from the G-B due to changing intensity of the SW monsoon (Kudrass et al., 2001, and Figure 1). The  $\delta^{18}\text{O}_{\text{SW}}$  record in SK 157-20 (this study; Figure 2c), although downstream from 126 KL, correlates with its salinity record (Figure 2d). Thus, it is reasonable to interpret the  $\delta^{18}\text{O}_{\text{SW}}$  record in SK 157-20 to reflect G-B outflow as the SW monsoon intensity varied. Besides, the  $\delta^{18}\text{O}$  record from SK 157-20 is in agreement with all other  $\delta^{18}\text{O}$  records in and around the central BoB (eg. Rashid et al., 2007; Marzin et al., 2013; Sijinkumar et al., 2016) as well as the Hulu Cave record (Wang et al., 2001). All of them indicate a weak SW monsoon during HS1 and intensification during the B-A. The YD period in the BoB has been reported to be a time of weakened SW monsoon (e.g., Kudrass et al., 2001), however, our sampling resolution is low for the YD and we refrain from making any strong interpretation for it. The sharp decrease in  $\delta^{18}\text{O}_{\text{SW}}$  at the end of the YD in SK157-20 marks the increased rainfall that has been reported previously by several researchers as the Holocene intensification of the SW monsoon (Sirocko et al., 1993; Naidu and Malmgren, 1996; Sinha et al., 2005; Rashid et al., 2007). Thus, the central BoB sea surface oxygen isotopes faithfully

record the regional SW monsoon precipitation and associated river discharge patterns. Moreover, the  $\delta^{18}\text{O}_{\text{sw}}$  record of SK 157-20 also correlates well with the  $\delta^{18}\text{O}$  record from the Greenland ice core NGRIP, which reflects Greenland air temperatures (Figure 2e; Svensson et al., 2008).

#### 6.1 Nd isotope time series in the central BoB: water mass vs. monsoon tracer

The surface BoB shows a dominant monsoonal influence in the present-day and the Holocene and is likely to receive abundant riverine contributions during strong monsoonal intervals in the past. Previous studies in the Indian Ocean that used Nd isotopes in foraminifera and sediments have concluded that changes in the riverine input of Nd, and/or changes in particulate sources, and/or changes in ocean circulation, can play a role in the Nd isotopic variations there (e.g., Burton and Vance, 2000; Stoll et al., 2007; Piotrowski et al., 2009; Wilson et al., 2015). In general the effects of surface particles on seawater Nd isotopes are mostly confined to the surface layers of the oceans, with little to no impact on bottom water values (e.g., Goldstein and Hemming, 2003; Bayon et al., 2003; Carter et al., 2012). Assuming that oxidative reductively cleaned planktic foraminifera represents the surface  $\epsilon_{\text{Nd}}$  seawater signal, Stoll et al. (2007) interpreted authigenic  $\epsilon_{\text{Nd}}$  data from the BoB as reflecting a shift in the riverine load of Nd from less radiogenic Himalayan terrains during the Holocene (via the G-B) to more radiogenic Burman Arc terrains during the Last Glacial Maximum (LGM), via southeast Asian rivers along the Arakan coast. They suggested this reflected different positions for the SW monsoon and the Inter-Tropical Convergence Zone (ITCZ) during the LGM compared to the Holocene, with the SW monsoon centered in the Indo-Burma region rather than the Indo-Gangetic plain, and the ITCZ located farther to the south. While later studies have demonstrated that the planktic foraminifera derived  $\epsilon_{\text{Nd}}$  data reported by Stoll et al. (2007) represent bottom water values (Tachikawa et al., 2013), the roles of the shifting locus of SW monsoon, and its effects on Nd released into the BoB from riverine particulates, along with the deglacial seawater Nd isotopic evolution of the BoB, warrant further evaluation.

Core MD77-176, situated close to SE Asian river runoff (Figure 1a, at 10.2°N, 95.05°E; 1375m), is suitably located to track the influence of fresh water and detrital particulate input from the Indo-Burman region associated with changes in the location of the SW monsoon. Such a shift of the SW monsoon would be indicated by increased fresh water flux from the SE Asian rivers and a decrease in sea surface salinity in core MD77-176. Comparison of the  $\delta^{18}\text{O}$  of the *G. ruber* record from MD77-176, a surface salinity indicator in the BoB, with that of a northern BoB core (126 KL) off the G-B river, shows a similar pattern of change over the entire deglaciation, suggesting comparable monsoonal activity in these two locations (Figure 3a).

The  $\epsilon_{Nd}$  end members of particulates from regional rivers can be grouped into two types, the G-B type, and the SE Asian river load-type draining the Indo-Burman ranges. The range of  $\epsilon_{Nd}$ -values of these end-members varies between the  $\epsilon_{Nd} = \sim -15$  off G-B rivers and  $\epsilon_{Nd} = \sim -8.7$  to  $-4$  off SE Asian rivers along the Arakan coast (Goldstein et al. 1984, Dia et al., 1992, Allen et al., 2008, Miriyala et al., 2017). The Holocene detrital  $\epsilon_{Nd}$  record in MD77-176 likely represents a mixture of G-B and SE Asian river sediments, and shows a gradual increase in  $\epsilon_{Nd}$ -values during the last deglaciation (Figure 3b) (Colin et al., 2006). If the detritus were the main contributing factor controlling the deglacial hydrogenous  $\epsilon_{Nd}$  evolution of central BoB, we would expect to observe similar pattern of changes in the  $\epsilon_{Nd}$  time series of MD77-176 and SK 157-20 with increases in the  $\epsilon_{Nd}$ -values. However, in SK157-20,  $\epsilon_{Nd}$ -values become progressively more negative across the deglaciation interval, indicating that Indo-Burman particulates cannot explain the seawater changes in the central BoB. Recently Yu et al. (2018) reported that the deglacial hydrogenous  $\epsilon_{Nd}$  in MD77-176 do not follow the observed changes in the detrital values. If the hydrogenous  $\epsilon_{Nd}$ -values in MD77-176 have not been affected by the particulate contributions from the proximal SE Asian Rivers, it is less likely that the Nd isotopic record of a more distal core in the central BoB would experience modification due to particulate discharge from these same rivers.

Surface ocean circulation patterns of Andaman Sea change between the summer and winter monsoons, however, fine-grained net sediment transport off the major SE Asian rivers is toward the south throughout the year, away from the BoB (Huang et al., 1997; Colin et al., 1999; Rizal et al., 2012). Thus, voluminous transport of suspended sediment from the Indo-Burman ranges to the central BoB is unlikely, and we can rule out the effect of Nd released from the SE Asian River borne particulates as a primary agent that can affect the bottom water in the central BoB.

It has been suggested that the  $\epsilon_{Nd}$ -values of modern day northern and central BoB bottom waters, as well as Holocene values from SK 157-20, are modified by Nd released from G-B particulates (e.g. Singh et al., 2012; Yu et al., 2017). In contrast, the late Holocene core top Nd isotopes in core SK 129-CR2 (Figure 1a) located in the equatorial Indian Ocean (Piotrowski et al., 2012), represents water mass mixing and can be considered as de-coupled from regional monsoonal influence (Wilson et al., 2015). For the time interval encompassing the last deglaciation, the  $\epsilon_{Nd}$  record of SK 157-20 agrees within error with the authigenic record from equatorial Indian Ocean core SK 129-CR2 (Figure 4a) (Piotrowski et al., 2009). SK 129-CR2 is distant from our study site (Figure 1), and yet these two records agree between  $\sim 16$  and  $8$  ka, indicating the deglacial central BoB  $\epsilon_{Nd}$  record represents a basin wide signal and does not reflect the G-B particulate load, which would establish a north-south gradient as observed in the present-day. For the same time interval, other BoB authigenic  $\epsilon_{Nd}$  times series,



located north and south of our study site and representing Circumpolar Deep Water (CDW) (Figure 4a), show good agreement and co-evolution with SK 157-20, further supporting a basin wide phenomenon. Thus, we conclude that during weak monsoon periods (compared to the Holocene), release of Nd to the bottom water from G-B particulates is decreased, reflecting lower amounts of G-B particulates, and as a result the  $\epsilon_{Nd}$  signature is dominated by water mass mixing.

## 6.2 State of deep ocean circulation in the central BoB during intervals of low monsoonal activity

In the modern ocean, NADW has an  $\epsilon_{Nd}$ -value of -13.5 near its sources in the North Atlantic (Piepgras and Wasserburg, 1987), whereas by the time it reaches the far South Atlantic and flows into the Indian Ocean toward the central BoB it has been modified by mixing with Southern Ocean waters, and the modified NADW (MNADW) has  $\epsilon_{Nd}$  of  $\sim -10$  to  $-12$  (Stichel et al. 2012, Garcia-Solsona et al. 2014). The other major Nd contributor to the BoB deep/abyssal waters is Antarctic Bottom Water (AABW), which forms at multiple locations around Antarctica with variable characteristic  $\epsilon_{Nd}$ -values (e.g., Ross Sea Bottom Water  $\sim -7$  (Basak et al., 2015); and Weddell Sea Bottom Water  $\sim -9.6$  (Stichel et al., 2012)). However, these ‘different AABWs’ are restricted to their respective formation basins and rarely cross the Polar Front without losing their initial Nd isotopic signature and attaining CDW  $\epsilon_{Nd}$  signatures (Basak et al., 2015). Deep CDW in different sectors of the Southern Ocean has nearly uniform  $\epsilon_{Nd}$ -values of  $\sim -8$  (Goldstein and Hemming, 2003; Stichel et al., 2012; Carter et al., 2012; Rickli et al., 2014; Basak et al., 2015). Fluctuating  $\epsilon_{Nd}$ -values of CDW in the past have been interpreted to mainly reflect changes in the NADW influx to the Southern Ocean (Piotrowski et al., 2005, 2008, 2009). Unlike AABW, NADW can be tracked for long distances, as is evident by the report of remnant NADW  $\epsilon_{Nd}$  signatures even at the far end of the meridional overturning circulation pathway in the southwestern Pacific (Molina-Kescher et al., 2014). Thus, in the context of  $\epsilon_{Nd}$  isotopes, the  $\epsilon_{Nd}$  evolution in the deep central BoB can be considered as being controlled by modified MNADW.

During HS1 the SK 157-20 record shows  $\epsilon_{Nd}$ -values consistently around  $\sim -7.6$  (Figure 2), indicating less MNADW export than during the Holocene and the YD. This observation is consistent with the Pa/Th record of NADW production, which was particularly weak during HS1 (McManus et al., 2004). Glacial-interglacial and millennial-scale variations in  $\epsilon_{Nd}$ -values in the deep South Atlantic have been shown to align with changes in Northern Hemisphere climate and interpreted to reflect changes in NADW export to the Southern Ocean (Piotrowski et al., 2005). As NADW production increased during the B-A, synchronous changes toward more negative  $\epsilon_{Nd}$ -values are observed in the Cape Basin  $\epsilon_{Nd}$  record (Piotrowski et al., 2004, 2005); and a gradual decrease in  $\epsilon_{Nd}$ -values is also observed in SK 157-20 (Figure 4b), albeit a bit delayed by  $\sim 500$  years, possibly due to long travel path of NADW from its source to the central BoB. For the rest of the B-A, SK 157-20 follows the NADW

record as reported in the western north Atlantic (Figure 4c; McManus et al., 2004, Roberts et al., 2010). Following the YD, until  $\sim 8$  ka, the  $\epsilon_{Nd}$ -value remained constant at around  $\sim -9$ , consistent with mixing between MNADW and Southern Ocean water. Thus, while the monsoonal changes controlled the surface hydrology in the central BoB, the deep water changes during the deglaciation were dominantly controlled by changes in the global overturning circulation.

There is an offset in authigenic  $\epsilon_{Nd}$  values between the deep records in the BoB and intermediate depth core MD77-176 near the Irrawaddy River mouth (Figure 1a) during the deglaciation, nevertheless the overall pattern of change throughout the entire period studied is similar, and the values during the LGM and Holocene are the same (Figure 3). The differences during the deglaciation might be attributed to the inherent differences in  $\epsilon_{Nd}$  values between intermediate and deep water masses bathing the BoB.

### 6.3 Transition from deep ocean circulation to monsoon dominated basin

Starting after  $\sim 8$  ka, the  $\epsilon_{Nd}$  record shows a second decrease in the  $\epsilon_{Nd}$ -value to  $\sim -10.5$ , which does not correspond to changes in the global overturning circulation. While the SW monsoon started intensifying at the onset of Holocene (at  $\sim 10$  ka), it was not until  $\sim 8$  ka that it reached its maximum (Kudrass et al., 2001). Between  $\sim 10$ -8 ka the sediment load from the adjoining G-B Rivers underwent a major increase (Goodbred and Kuehl, 2000). The time period leading to the SW monsoon maximum (11-8 kyr) was also a period of a steep sea level rise (e.g. Lambeck et al., 2014), which flooded the Bengal margin and inhibited the transfer of sediments load to the deep ocean (Goodbred and Kuehl, 2000). Following  $\sim 7$  ka, sea level stabilized (Lambeck et al., 2014), coincident with the shift to more negative  $\epsilon_{Nd}$ -values in SK 157-20 and subsequent stabilization at  $\sim -10.5$ , offset from the equatorial Indian Ocean core SK 129-CR2 (Figures 1a, 2, 4a). The coeval decoupling of central BoB  $\epsilon_{Nd}$  record at  $\sim 8$  ka from the equatorial Indian Ocean deep waters at the time of sea level stabilization indicates that the sediment had filled the margin sufficiently such that sediment reaching the deep BoB began to affect to the deep waters'  $\epsilon_{Nd}$  signature (Singh et al., 2012; Yu et al., 2017).

## 6. Conclusions

Many past climate change signals in the Indian Ocean are overprinted by the Indian monsoon. Our Nd isotope down core record from the deep central BoB indicates that the global overturning circulation controlled the deep water  $\epsilon_{Nd}$  signature there for the major part of the deglaciation, until  $\sim 8$  ka. The reconstructed deep circulation history during the deglacial is in agreement with the NADW production history and its export to the Southern Ocean. Since  $\sim 8$ -7 ka, intensification of SW monsoon increased riverine particulates (primarily from the G-B) which released Nd and dominated the

hydrogenous  $\epsilon_{Nd}$  signal in the deep central BoB, leading up to the modern conditions where the Nd isotopes there are strongly impacted by the monsoon.

### **Acknowledgements**

Nd isotopic analyses were funded jointly by the CSIR-NIO GEOSINKS program grant to SN and a LDEO Climate Center grant to CB and SG. Funding for AMS dates was obtained from a MoES grant to PDN. The authors thank Louise Bolge for assistance in the lab. All of the data can be found in Table 1. This is National Institute of Oceanography contribution number XXXX and LDEO contribution number XXXX.

## References

- Allen, R., Najman, Y., Carter, A., Barford, D., Bickle, M.J., Chapman, H.J., Garzanti, E., Vezzoli, G., Ando, S. & Parrish, R.R. (2008). Provenance of the Tertiary sedimentary rocks of the Indo-Burman Ranges, Burma (Myanmar): Burman arc or Himalayan-derived? *Journal Geological Society London*, 165, 1045–1057. <https://doi.org/10.1144/0016-76492007-143>
- Basak, C., Pahnke, K., Frank, M., Lamy, F., & Gersonde, R. (2015). Neodymium isotopic characterization of Ross Sea Bottom Water and its advection through the southern South Pacific. *Earth and Planetary Science Letters*, 419, 211-221. <http://dx.doi.org/10.1016/j.epsl.2015.03.011>
- Bayon, G., German, C. R., Nesbitt, R. W., Bertrand, P., & Schneider, R. R. (2003). Increased input of circumpolar deep water-borne detritus to the glacial SE Atlantic Ocean. *Geochemistry Geophysics Geosystem*, 4(3), 1025. <https://doi.org/10.1029/2002GC000371>, 2003
- Burton, K.W., & Vance, D. (2000) Glacial–interglacial variations in the neodymium isotope composition of seawater in the Bay of Bengal recorded by planktonic foraminifera. *Earth and Planetary Science Letters*, 176 (3–4), 425–441.
- Carter, P., Vance, D., Hillenbrand, C. D., Smith, J. A., & Shoosmith D. R. (2012). The neodymium isotopic composition of waters masses in the eastern Pacific sector of the Southern Ocean. *Geochimica et Cosmochimica Acta*, 79, 41–59. <https://doi.org/10.1016/j.gca.2011.11.034>
- Colin, C., Turpin, L., Bertaux, J., Desprairies, A., & Kissel, C. (1999). Erosional history of the Himalayan and Burman ranges during the last two glacial-interglacial cycles. *Earth and Planetary Science Letters*, 171, 647-660.
- Colin, C., Turpin, L., Blamart, D., Frank, N., Kissel, C., & Duchamp, S. (2006). Evolution of weathering patterns in the Indo-Burman Ranges over the last 280 kyr: Effects of sediment provenance on  $^{87}\text{Sr}/^{86}\text{Sr}$  ratios tracer. *Geochemistry Geophysics Geosystem*, 7, Q03007. <https://doi.org/10.1029/2005GC000962>
- Dia, A., Dupre, B., & Allegre C.J. (1992). Nd isotopes in Indian Ocean sediments used as a tracer of supply to the ocean and the circulation pathways. *Marine Geology*, 103, 349–459.
- Duplessy, J.C. (1982). Glacial to interglacial contrasts in the northern Indian Ocean. *Nature*, 295, 494-498.
- Garcia-Solsona, E., Jeandel, C., Labatut, M., Lacan, F., Vance, D., Chavagnac, V., & Pradoux, C. (2014). Rare earth elements and Nd isotopes tracing water mass mixing and particle–seawater interactions in the SE Atlantic. *Geochimica et Cosmochimica Acta*, 125, 351–372. <https://doi.org/10.1016/j.marchem.2015.03.011>
- Goldstein, S.L., O’Nions, R.K., & Hamilton, P.J. (1984) A Sm-Nd isotopic study of atmospheric dusts and particulates from major river systems. *Earth and Planetary Science Letters*, 70, 221-236.

- Goldstein, S.L., & Hemming, S.R. (2003). Long-lived isotopic tracers in oceanography, paleoceanography and ice sheet dynamics. *In: Elderfield, H. (Ed.), Treatise on Geochemistry: Elsevier, Oxford*, 453–489.
- Goodbred, J.S.L., & Kuehl, S.A. (2000). Enormous Ganges-Brahmaputra sediment discharge during strengthened early Holocene monsoon. *Geology*, 28 (12), 1083-1086. [https://doi.org/10.1130/0091-7613\(2000\)28<1083:EGSDDS>2.0.CO;2](https://doi.org/10.1130/0091-7613(2000)28<1083:EGSDDS>2.0.CO;2)
- Gourlan, A. T., Meynadier, L., Allègre, C.J., Tapponnier, P., Birck, J-L., & Joron, J-L. (2010). Northern Hemisphere climate control of the Bengali rivers discharge during the past 4 Ma. *Quaternary Science Reviews*, 29, 2484-2498. <https://doi.org/10.1016/j.quascirev.2010.05.003>.
- Govil, P., & Naidu P. D. (2011). Variations of Indian monsoon precipitation during the last 32 kyr reflected in the surface hydrography of the Western Bay of Bengal. *Quaternary Science Reviews*, 30, 3871-3879. <https://doi.org/10.1016/j.quascirev.2011.10.004>
- Huang, C.Y., Liew, P.M., Zhao, M., Chang, T.Z., Kuo, C.M., Chen, M.T., Want, C.H., & Zheng L.F. (1997). Deep sea and lake records of the Southeast Asian paleomonsoons for the last 25 thousands years. *Earth and Planetary Science Letters*, 146, 59–72.
- Jacobsen, S.B., & Wasserburg, G.J. (1980). Sm-Nd evolution of chondrites. *Earth and Planetary Science Letters*, 50 (1980) 139-155.
- Kudrass, H.R., Hofmann, A., Doose, H., Emeis, K., & Erlenkeuser, H. (2001). Modulation and amplification of climatic changes in the Northern Hemisphere by the Indian summer monsoon during the past 80 k.y. *Geology*, 29, 63-66. [https://doi.org/10.1130/0091-7613\(2001\)029<0063:MAAOCC>2.0.CO;2](https://doi.org/10.1130/0091-7613(2001)029<0063:MAAOCC>2.0.CO;2)
- Kumar, M.D., & Li, Y.H. (1996). Spreading of water masses and regeneration of silica and  $^{226}\text{Ra}$  in the Indian Ocean. *Deep-Sea Research II*, 43, 83-110. [https://doi.org/10.1016/0967-0645\(95\)00084-4](https://doi.org/10.1016/0967-0645(95)00084-4)
- Lambeck, K., Rouby, H., Purcell, A., Sun, Y., & Sambridge, M. (2014). Sea level and global ice volumes from the Last Glacial Maximum to the Holocene. *Proceedings of the National Academy of Sciences, U.S.A.*, 111, 15296-15303. <https://doi.org/10.1073/pnas.1411762111>
- Martin, E.E., & Scher, H.D. (2004). Preservation of seawater Sr and Nd isotopes in fossil fish teeth: bad news and good news. *Earth Planet. Science Letters*, 220 (1-2), 5–39. [https://doi.org/10.1016/S0012-821X\(04\)00030-5](https://doi.org/10.1016/S0012-821X(04)00030-5)
- Marzin, C., Kallel, N., Kageyama, M., Duplessy, J. C., & Braconnot, P. (2013). Glacial fluctuations of the Indian monsoon and their relationship with North Atlantic climate: new data and modelling experiments. *Climate of the Past*, 9, 2135–2151. <https://doi.org/10.5194/cp-9-2135-2013>

- McManus, J.F., Francois, R., Gherardi, J.M., Keigwin, L.D., & Leger, S.B. (2004). Collapse and rapid resumption of Atlantic meridional circulation linked to deglacial climate changes. *Nature*, 428, 834-837. <https://doi.org/10.1038/nature02494>
- Miriyala, P., Sukumaran, N.P., Nath, B.N., Ramamurty, P.B., Sijinkumar, A.V., Vijayagopal, B., Ramaswamy, V., & Sebastian, T. (2017). Increased chemical weathering during the deglacial to mid-Holocene summer monsoon intensification. *Scientific Reports*, 7, 44310. <https://doi.org/10.1038/srep44310>
- Molina-Kescher, M., Frank, M., & Hathorne, E. (2014). South Pacific dissolved Nd isotope compositions and rare earth element distributions: water mass mixing versus biogeochemical cycling. *Geochimica et Cosmochimica Acta*, 127, 171–189. <https://doi.org/10.1016/j.gca.2013.11.038>
- Naidu, P.D., & Malmgren, B.A. (1996). A high-resolution record of late Quaternary upwelling along the Oman Margin, Arabian Sea based on planktonic foraminifera. *Paleoceanography*, 11, 129-140.
- Naik, S. S., & Naidu, P. D. (2016). Carbonate preservation during the ‘mystery interval’ in the northern Indian Ocean. *Geochemical Journal*, 50, 357-362, <https://doi.org/10.2343/geochemj.0420>.
- Pena, L. D., Goldstein, S. L., Hemming, S. R., Jones, K. M., Calvo, E., Pelejero, C., & Cacho, I. (2013). Rapid changes in meridional advection of Southern Ocean intermediate waters to the tropical Pacific during the last 30 kyr. *Earth and Planetary Science Letters*, 368, 20–32. <https://doi.org/10.1016/j.epsl.2013.02.028>
- Piegras, D. J., and Wasserburg, G. J., 1987, Rare earth element transport in the western North Atlantic inferred from Nd isotopic observations, *Geochimica et Cosmochimica Acta*, v. 51, p.1257–1271.
- Piotrowski, A. M., Goldstein, S. L., Hemming, S. R., & R. G. Fairbanks (2004). Intensification and variability of ocean thermohaline circulation through the last deglaciation. *Earth and Planetary Science Letters*, 225(1–2), 205–220. <https://doi.org/10.1016/j.epsl.2004.06.002>
- Piotrowski, A.M., Goldstein, S.L., Hemming, S.R., & Fairbanks, R.G. (2005). Temporal relationships of carbon cycling and ocean circulation at glacial boundaries. *Science*, 307 (5717), 1933–1938. <https://doi.org/10.1016/j.epsl.2009.06.007>
- Piotrowski, A.M., Goldstein, S.L., Hemming, S.H., Fairbanks, R.G., & Zylberberg, D.R. (2008). Oscillating glacial northern and southern deep water formation from combined neodymium and carbon isotopes. *Earth and Planetary Science Letters*, 272, 394–405. <https://doi.org/10.1016/j.epsl.2008.05.011>
- Piotrowski, A.M., Banakar, V.K., Scrivner, A.E., Elderfield, H., Galy, A., & Dennis, A. (2009). Indian Ocean circulation and productivity during the last glacial cycle. *Earth and Planetary Science Letters*, 285, 179–189. <https://doi.org/10.1016/j.epsl.2009.06.007>

- Piotrowski, A. M., Galy, A., Nicholl, J. A. L., Roberts, N., Wilson, D. J., Clegg, J. A., & Yu, J. (2012). Reconstructing deglacial North and South Atlantic deep water sourcing using foraminiferal Nd isotopes. *Earth and Planetary Science Letters*, 357–358, 289–297. <https://doi.org/10.1016/j.epsl.2012.09.036>
- Rashid, H., Flower, B.P., Poore, R.Z., & Quinn, T.M. (2007). A ~ 25 ka Indian Ocean monsoon variability record from the Andaman Sea. *Quaternary Science Reviews*, 26, 2586–2597. <https://doi.org/10.1016/j.quascirev.2007.07.002>
- Rickli, J., Gutjahr, M., Vance, D., Fischer-Godde, M., Hillenbrand, C.-D., & Kuhn G. (2014). Neodymium and hafnium boundary contributions to seawater along the West Antarctic continental margin. *Earth and Planetary Science Letters*, 394, 99–110. <https://doi.org/10.1016/j.epsl.2014.03.008>
- Rizal, S., Damm, P., Wahid, M.A., Sundermann, J., Ilhamsyah, Y., Iskandar, T., & Muhammad (2012). General circulation in the Malacca Strait and Andaman Sea: A numerical model study. *American Journal of Environmental Sciences*, 8, 479–488. <https://doi.org/10.3844/ajessp.2012.479.488>
- Roberts, N. L., Piotrowski, A. M., McManus, J. F. & Keigwin, L. D. (2010). Synchronous deglacial overturning and water mass source changes. *Science*, 327, 75–78. <https://doi.org/10.1126/science.1178068>.
- Schlitzer, R. (2015). Data Analysis and Visualization with Ocean Data View, *CMOS Bulletin SCMO*, 43, 1, 9-13. [hdl:10013/epic.45187](https://doi.org/10.10013/epic.45187)
- Schulz, H., von Rad, U., & Erlenkeuser, H. (1998). Correlations between Arabian Sea and Greenland climate oscillations of the past 110,000 years. *Nature*, 393, 54–57.
- Sengupta, D., Bharath Raj, G. N., & Shenoi S. S. C. (2006). Surface freshwater from Bay of Bengal runoff and Indonesian Throughflow in the tropical Indian Ocean. *Geophysical Research Letters*, 33, L22609, <https://doi.org/10.1029/2006GL027573>.
- Singh, S.P., Singh, S.K., Goswami, V., Bhushan, R., & Rai, V.K. (2012). Spatial distribution of dissolved neodymium and  $\epsilon\text{Nd}$  in the Bay of Bengal: Role of particulate matter and mixing of water masses. *Geochimica et Cosmochimica Acta*, 94, 38–56. <https://doi.org/10.1016/j.gca.2012.07.017>
- Sinha, A., Cannariato, K. G., Stott L. D., Li, H.-C., You, C.-F., Cheng, H., Edwards, R. L., & Singh, I. B. (2005). Variability of southwest Indian summer monsoon precipitation during the Bølling-Allerød. *Geology*, 33, 813 – 816. <https://doi.org/10.1029/2007GL030431>
- Sirocko, F., Sarnthein, M., Erlenkeuser, H., Lange, H., Arnold, M., & Duplessy, J.C. (1993). Century scale events in monsoon climate over the past 24,000 years. *Nature*, 364, 322–324.
- Stichel, T., Frank, M., Rickli, J., & Haley, B. A. (2012). The hafnium and neodymium isotope composition of seawater in the Atlantic sector of the Southern Ocean. *Earth and Planetary Science Letters*, 317, 282–294. <https://doi.org/10.1016/j.epsl.2011.11.025>

- Stoll, H.M., Vance, D., & Arevalos, A. (2007). Records of the Nd isotope composition of seawater from the Bay of Bengal: Implications for the impact of Northern Hemisphere cooling on ITCZ movement. *Earth and Planetary Science Letters*, 255, 213–228. <https://doi.org/10.1016/j.epsl.2006.12.016>
- Svensson, A., Andersen, K.K., Bigler, M., Clausen, H.B., Dahl-Jensen, D., Davies, et al. (2008). A 60000 year Greenland stratigraphic ice core chronology. *Climate of the Past*, 4, 47–57, <https://doi.org/10.5194/cp-4-47-2008>
- Tanaka, T., Togashi, S., Kamioka, H., Amakawa, H., Kagami, H., Hamamoto, T. et al. (2000). Ndi-1: a neodymium isotopic reference in consistency with La Jolla neodymium. *Chemical Geology*, 168, 279–281. [https://doi.org/10.1016/S0009-2541\(00\)00198-4](https://doi.org/10.1016/S0009-2541(00)00198-4)
- van de Flierdt, T., Griffiths, A.M., Lambelet, M., Little, S.H., Stichel, T., & Wilson, D.J. (2016). Neodymium in the oceans: a global database, a regional comparison and implications for palaeoceanographic research. *Philosophical Transactions of the Royal Society of London. Series A, Mathematical Physical and Engineering Sciences*, 374, 2081, <https://doi.org/10.1098/rsta.2015.0293>
- Wang, Y.J., Cheng, H., Edwards, R.L., An, Z.S., Wu, J.Y., Shen, C.C., & Dorale, J.A. (2001). A high-resolution absolute-dated Late Pleistocene Monsoon record from Hulu Cave, China. *Science*, 294, 2345-2348. <https://doi.org/10.1126/science.1064618>
- Wilson, D.J., Piotrowski, A. M., Galy, A., & McCave, I.N. (2012). A boundary exchange influence on deglacial neodymium isotope records from the deep western Indian Ocean. *Earth and Planetary Science Letters*, 341-344, 35-47, <https://doi.org/10.1016/j.epsl.2012.06.009>
- Wilson, D.J., Piotrowski, A. M., Galy, A., & Banakar, V. K. (2015). Interhemispheric controls on deep ocean circulation and carbon chemistry during the last two glacial cycle. *Paleoceanography*, 30, 621-641. <https://doi.org/10.1002/2014PA002707>
- Wyrski, K. (1973). An Equatorial Jet in the Indian Ocean. *Science*, 181, 262-264. <https://doi.org/10.1126/science.181.4096.262>
- Yu..Z., Colin, C., Meynadier, L., Douville, E., Dapoigny, A., Reverdin, G., Wu, Q., Wan, S., Song, L., Xu, Z., & Bassinot, F. (2017). Seasonal variations in dissolved Neodymium isotope composition in the Bay of Bengal. *Earth and Planetary Science Letters*, 479, 310-321. <https://doi.org/10.1016/j.epsl.2017.09.022>
- Yu..Z., Colin, C., Meynadier, L., & Wan, S. (2018). Antarctic Intermediate Water penetration into the Northern Indian Ocean during the last deglaciation. *Earth and Planetary Science Letters*, 500, 67-75. <https://doi.org/10.1016/j.epsl.2018.08.006>



**Table 1 Caption:  $\epsilon_{Nd}$  and  $\delta^{18}O$  (‰ VPDB) values from SK 157/20**

**Table 1**

Core	Depth (cm)	Age (ka)	Material	Normalized $^{143}\text{Nd}/^{144}\text{Nd}$	$\epsilon_{Nd}$	Internal error (2 SE $\epsilon_{Nd}$ units)	External error (2 $\sigma$ $\epsilon_{Nd}$ units)	$\delta^{18}O$ (G. <i>ruber</i> )
SK 157/20 ( 12°09'N; 88°42'E) (3171 m)	0-1	3.87						-2.52
	1-3	4.29	forams	0.512106	-10.4	0.21	0.30	-2.40
	3-4	4.50	forams	0.512100	-10.5	0.41	0.30	-2.25
	4-5	4.72	forams	0.512107	-10.4	0.16	0.30	-2.34
	5-6	4.93	forams	0.512097	-10.6	0.33	0.30	-2.38
	6-7	5.14	forams	0.512097	-10.6	0.36	0.17	-2.46
	7-8	5.35						-2.30
	8-9	5.57	forams	0.512099	-10.5	0.24	0.27	-2.49
	9-10	5.78						-2.82
	10-12	6.20	forams	0.512102	-10.5	0.25	0.30	-2.66
	12-14	6.63	forams	0.512096	-10.6	0.24	0.27	-2.75
	12-14	6.63	fish teeth	0.512091	-10.7	0.65	0.50	
	14-16	7.05	forams	0.512106	-10.4	0.15	0.30	-2.70
	16-18	7.47						-2.70
	18-20	7.90	forams	0.512169	-9.2	0.31	0.27	-2.91
	20-22	8.32	forams	0.512166	-9.2	0.47	0.30	-2.66
	22-24	8.75	forams	0.512178	-9.0	0.13	0.30	-2.61
	24-26	10.11	forams	0.512191	-8.7	0.25	0.30	-2.68
	26-28	11.46	forams	0.512182	-8.9	0.18	0.30	-1.84
	28-30	12.82	forams	0.512210	-8.4	0.19	0.30	-1.43
	30-32	13.13						-1.57
	32-34	13.44	forams	0.512248	-7.6	0.18	0.30	-1.26
	34-38	13.75						-1.95
	36-38	14.06	forams	0.512255	-7.5	0.24	0.30	-1.43
	38-40	14.37						-1.52
	40-42	14.68						-1.59
	42-44	14.99	forams	0.512147	-9.6	0.16	0.30	-0.87
	44-46	15.04	forams	0.512256	-7.5	0.23	0.30	-0.76
	46-48	15.10						-0.90
	48-50	15.16	forams	0.512234	-7.9	0.12	0.31	-0.91
50-52	15.22	forams	0.512243	-7.7	0.25	0.30	-0.84	
52-54	15.28	forams	0.512231	-7.9	0.21	0.30	-1.33	
60-62	15.51						-0.71	
62-64	15.56						-0.79	
64-66	15.62	forams	0.512275	-7.1	0.14	0.31	-0.99	

66-68	15.68	-0.69
68-70	15.74	-0.77
70-72	15.79	-0.84
72-74	15.85	-0.89

---

*Note.* <sup>a</sup>Analytical procedures are given in Materials and Methods.

## Figure captions:

**Figure 1.** Core locations and general hydrography of Bay of Bengal. (a) Location of core SK 157-20 (this study; 12°09'N; 88°42'E, water depth 3171 m) and other cores and hydrographic station (Singh et al., 2012) used for comparison are shown. Major rivers relevant to the study are also shown. (b) A south-north salinity section showing major water masses and relative position of cores from this study and literature are plotted. (CDW= Circumpolar Deep Water, AABW= Antarctic Bottom Water, and AAIW= Antarctic Intermediate Water). This figure was prepared using Ocean Data View (Schlitzer, 2015).

**Figure 2.** Surface and deep ocean climate proxy responses from central Bay of Bengal and Greenland covering periods of abrupt climate change events following the last deglaciation (16 - 4 kyr BP). (a) Nd isotopes (expressed as  $\epsilon_{Nd}$ :  $\epsilon_{Nd} = ((^{143}Nd/^{144}Nd_{measured}/^{143}Nd/^{144}Nd_{CHUR}) - 1) * 10^4$ ) of mixed planktic foraminifera species from SK 157-20, highlighting deep water circulation changes in the central BoB. Vertical error bars reflect external reproducibility of international standard JNdi-1 measured during the analytical session in which the sample was analyzed, except for samples with higher internal error. The filled cyan circle with an error bar represents the  $\epsilon_{Nd}$ -value derived from fossil fish debris. Climatic events are marked with shaded bars (YD = Younger Dryas; B-A = Bølling Allerød; HS1 = Heinrich Stadial 1). The red dashed line represents modern day bottom water  $\epsilon_{Nd}$ -value near the core location (Fig. 1; Singh et al., 2012). (b)  $\delta^{18}O$  (‰ PDB) record of *Globigerinoides ruber* from SK 157-20. (c)  $\delta^{18}O$  of seawater,  $\delta^{18}O_{sw}$ , derived from of SK 157-20 and Mg/Ca SST from another BoB sediment core, SK218 (Govil and Naidu, 2011). (d) Surface seawater salinity record from the northern BoB (126 KL, location in Fig. 1; Kudrass et al., 2001). (e)  $\delta^{18}O$  (‰ SMOW) from Greenland ice core, NGRIP (Svensson et al., 2008).

**Figure 3.** Comparison between  $\delta^{18}O$  of *G. ruber* and  $\epsilon_{Nd}$  inf sediment and hydrogenous materials in the BoB. (a)  $\delta^{18}O$  of *G. ruber*, showing the salinity evolution in the northern (SO93-126KL, Kudrass et al., 2001) and eastern BoB (MD77-176, Marzin et al., 2013) during the last deglaciation. (b) The deglacial sediment-derived  $\epsilon_{Nd}$  signature (MD77-176, Colin et al., 2006) evolved independently of the hydrogenous  $\epsilon_{Nd}$  signature in both the eastern (MD77-176, Yu et al., 2018) and central BoB (SK 157-20, this study)

**Figure 4.** Multi-proxy compilation of climate records following last deglaciation. (a)  $\epsilon_{Nd}$  records representing the central BoB (filled red squares, this study; SK157-20) and the equatorial Indian Ocean (filled black squares, Piotrowski et al., 2009; SK 129 CR2). Comparison with other hydrogenous  $\epsilon_{Nd}$  data north and south of our study sites show that the deep  $\epsilon_{Nd}$  signature of the BoB co-evolved during the last deglaciation. The red dashed line represents the modern day bottom water  $\epsilon_{Nd}$ -value near the core location (Singh et al., 2012). (b)  $\epsilon_{Nd}$  record of from the Cape Basin, South Atlantic (Piotrowski et al., 2005). (c)  $\epsilon_{Nd}$  (empty blue circles) and  $^{231}Pa/^{230}Th$  (filled violet squares) records from the North Atlantic (Roberts et al., 2010, McManus et al., 2004).

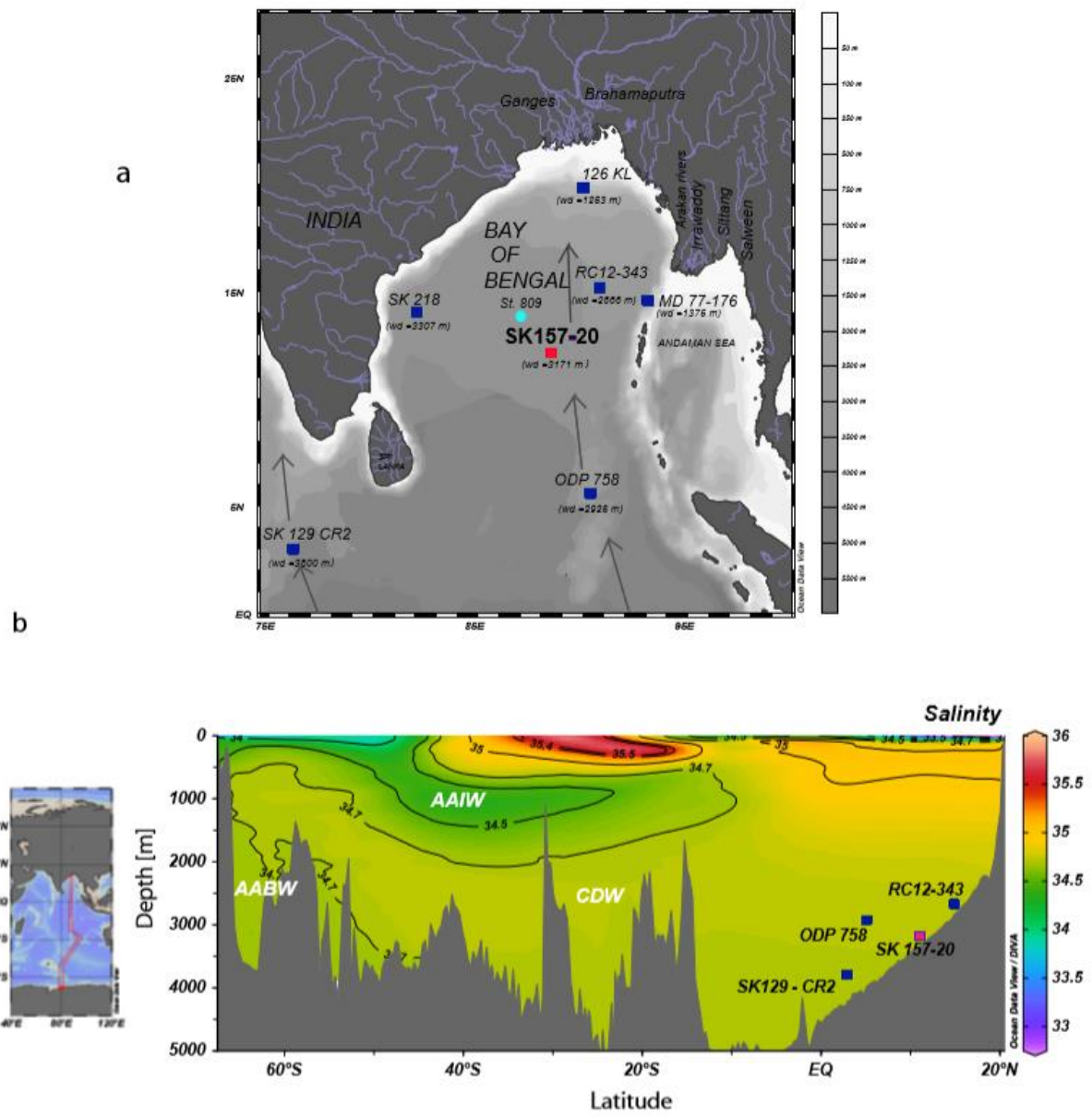


Figure 1

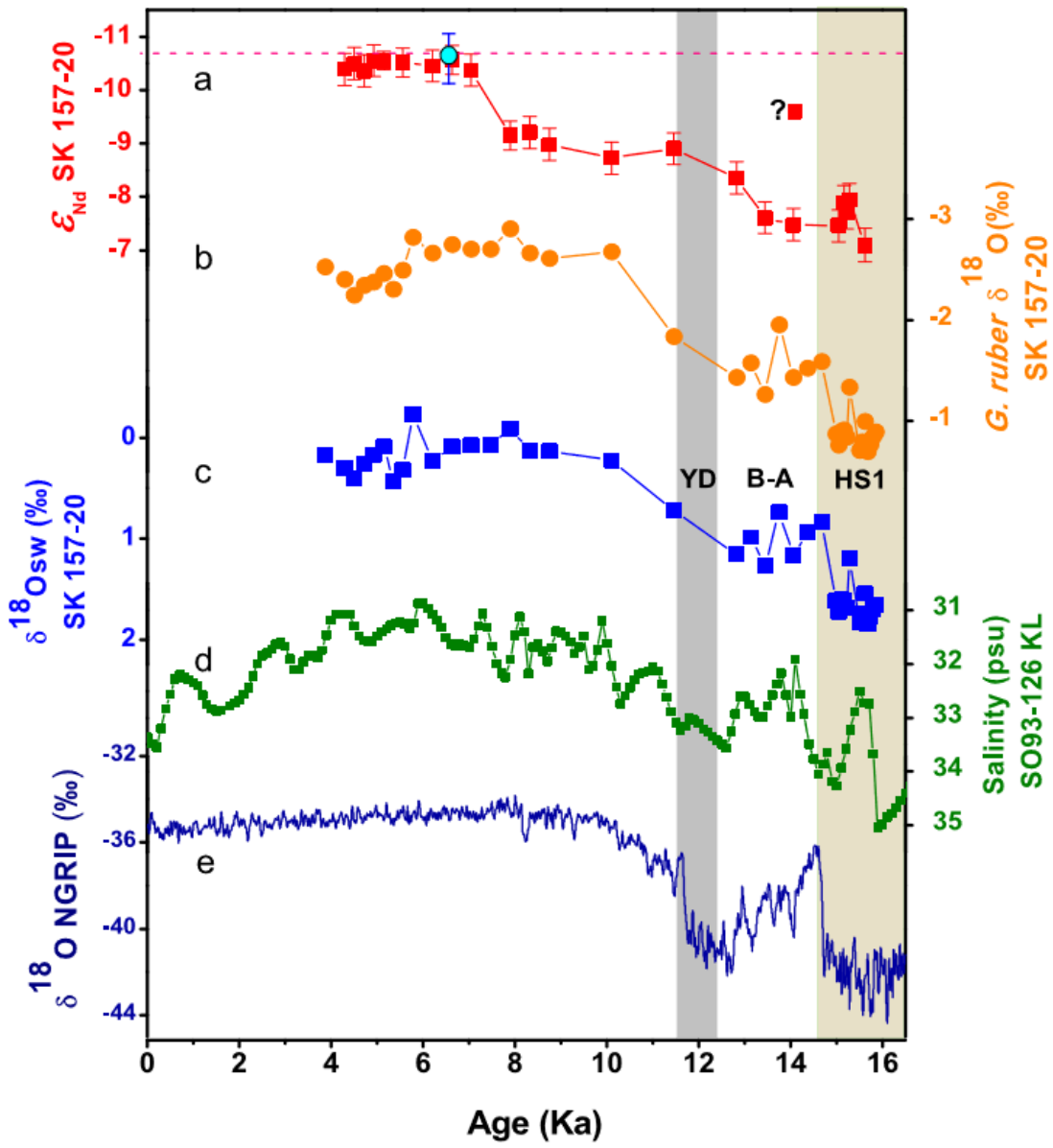


Figure 2

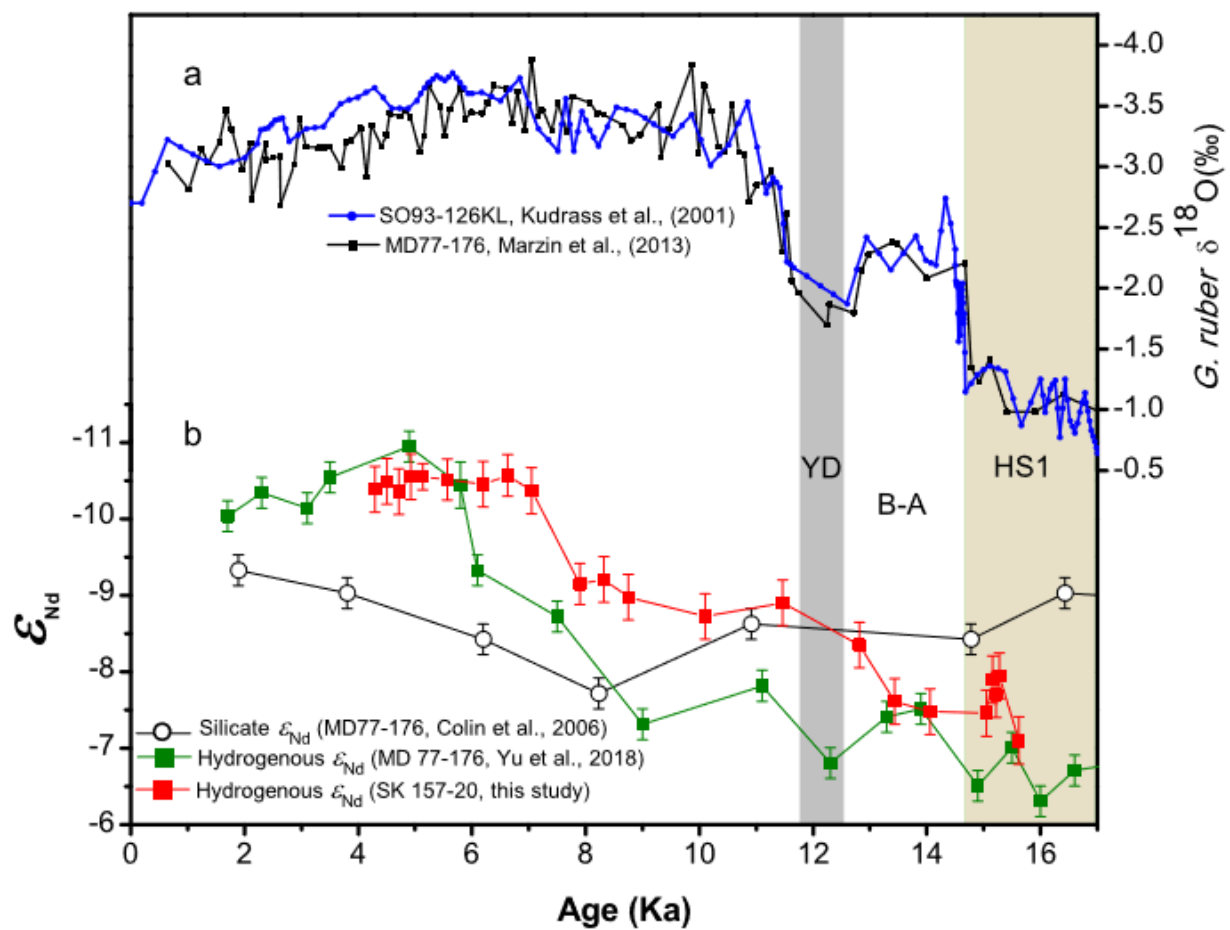


Figure 3

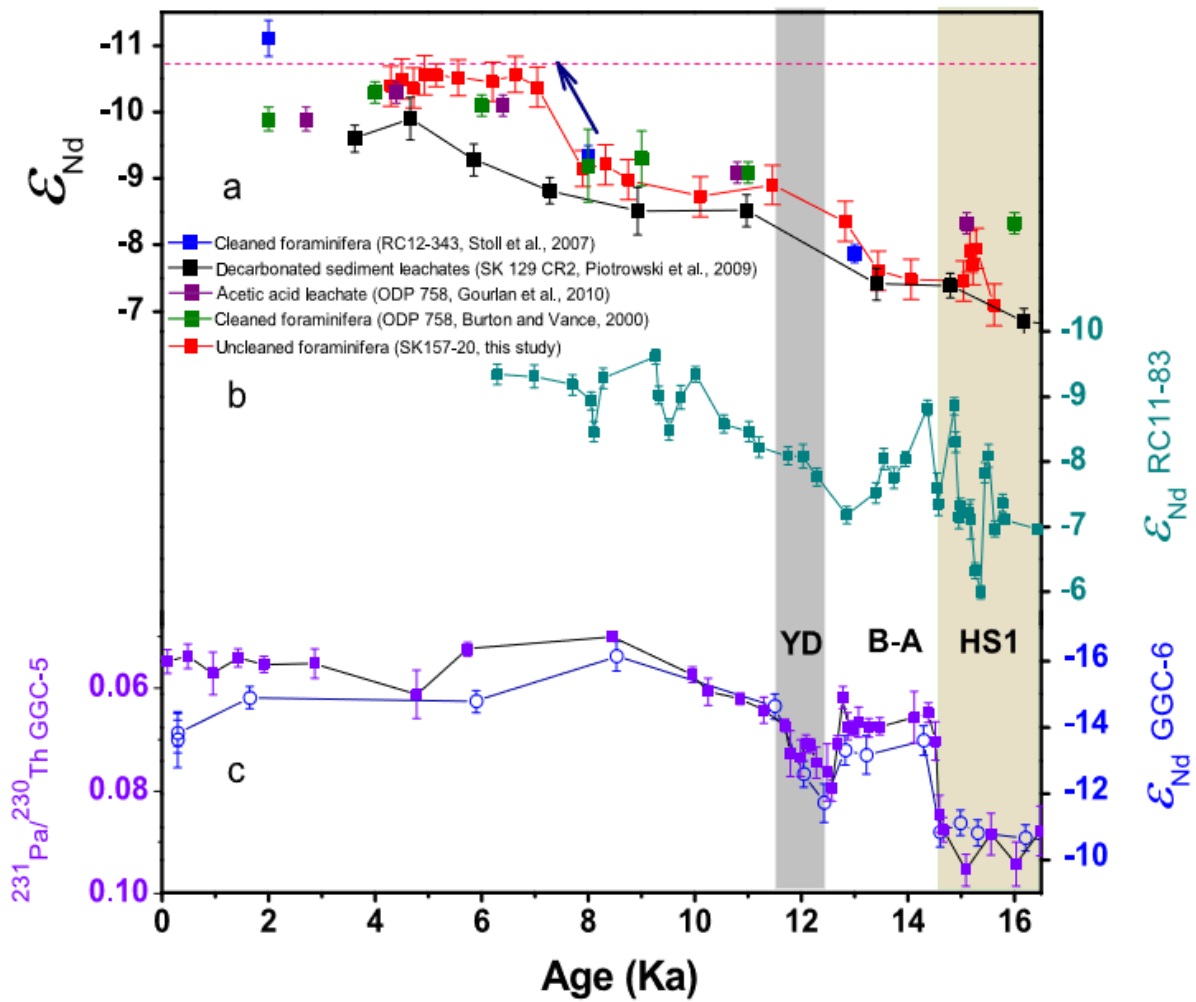


Figure 4